ASEE AMERICAN SOCIETY FOR ENGINEERING EDUCATION
ORIGINAL ARTICLE
Journal of Engineering Technology (ISSN: 0747-9964)
Volume 6. Issue 1. Jan. 2017. PP.35-48

Low Temperature Spark Plasma Sintered Irregular Shaped Ti6Al4V Powders with Enhanced Properties

A.O. Adegbenjo[a, *], E. Nsiah-Baafi[a], M.B. Shongwe[a], P.A. Olubambi[a, b] and J.H. Potgieter[c]

a. Institute for NanoEngineering Research, Department of Chemical, Metallurgical, and Materials Engineering, Tshwane University of Technology, PMB X 680, Pretoria 0001, South Africa.

b. Department of Chemical Engineering Technology, University of Johannesburg, Johannesburg 2006, South Africa.

c. School of Chemical and Metallurgical Engineering, University of The Witwatersrand, Johannesburg 2000, South Africa.

Abstract. The low temperature densification of large particle sized, prealloyed, and irregular shaped Ti6Al4V powders via the spark plasma sintering technique was explored in this work. This was aimed at lowering the high costs often associated with the processing of these alloy powders into bulk materials. Sintering of as-received powders were performed in vacuum at a constant heating rate, applied pressure and sintering temperature of 100 °C/min, 50 MPa and 850 °C respectively, while the holding time was varied from 2 to 10 min. Density and hardness measurements were according to Archimedes' principle and Vickers indentation method respectively. Characterization of the as-received powder, microstructural evolution studies, fractography and phase identification in the sintered alloys were achieved by scanning electron microscopy (SEM), energy dispersive X-ray spectrometry (EDX) and X-ray diffraction (XRD) techniques. Optimum properties in sintered samples was attained at 6 min holding time with 99.7 % relative density and Vickers micro-indentation hardness of 366 $HV_{0.1}$. The observed fracture modes in the sintered alloys were predominantly transgranular with characteristic fine dimples suggesting the samples were sintered to full densification. Hence, spark plasma sintering technique is affirmed as an economical and viable route for producing Ti6Al4V alloys with enhanced hardness and fracture characteristics.

Keywords: Titanium alloy**,** micro-hardness, densification, holding time, characterization.

1 Introduction

The high cost of producing titanium alloys via the conventional ingot metallurgy as compared to steel and aluminum limits their industrial applications [1]. Although, researchers have opined that utilizing a combination of low cost feedstock powder and cost-effective processing will, in the long run, lower the cost of production significantly [2]. Nevertheless, the powder metallurgy (P/M) route has been identified by many authors as a viable and promising cost-effective fabrication route for titanium alloys [3-7]. However, the characteristics of the feedstock powder (particle size, morphology, distribution, blended or prealloyed) among other factors influence the sintering behavior, density, microstructure and final mechanical properties of the sintered bulk material [8].

These characteristics of feedstock powders are determined by the method of powder production. Spherical powders usually obtained from gas or plasma atomization processes are used for advanced P/M techniques such as injection molding and hot isostatic pressing due to their high packing density and the

Journal of Engineering Technology (ISSN: 0747-9964)
Volume 6. Issue 1. Jan. 2017. PP.35-48

close proximity of particles [9, 10]. These kinds of powders contain less oxygen and as such lend themselves to high compressibility during handling and pressing operations.

On the other hand, irregular and angular shaped powders typical of the hydride-dehydride (HDH) processes are cheaper, with improved final shape retention due to their more textured surface and shape characteristics. However, they are seldom desired for P/M processes. This is due to their poor packing density, high porosity and increased friction between particles resulting to low flow rates and posing difficulty in achieving full densification during pre-sintering and compaction processes [9-12]. These types of powders also have high oxygen contents which make them difficult to deform while being compacted under uniaxially applied forces. They do experience high stress and small contact areas with the dies which subsequently lead to a fracturing of the specimens (or at times the die) during compaction [11]. These problems limit the use of irregular and angular shaped powders in P/M industrial applications despite their low cost which ought to be an advantage for their utilization.

Owing to the high affinity of titanium alloy powders (especially the irregular shaped) for oxygen and nitrogen, the mechanical properties of bulk materials sintered from these powders are compromised as a result of interstitial effects. Consequently, processing of these powders require sintering at high temperatures and vacuum to avoid interstitial impurities and reduce surface oxides thereby posing a tremendous setback to their applications due to high processing costs [2, 13].

The spark plasma sintering (SPS) technology, a very fast and efficient materials consolidation technique, which provides significant advantages of compressing and sintering of powders with poor deformability properties has recently been reported to be an effective technique for fabricating "hard to sinter" and irregular shaped titanium based powders [14-16]. Despite the number of reported studies on SPS processing of these powders, it is however observed that these studies are focused on the sintering of ultrafine-grained Ti6Al4V (Ti64) powders at high temperatures above 1000 °C. For example, it has been reported that a minimum of 1200 °C is required for Ti64 powders to attain the equivalent hardness of wrought products independent of the powder production method and it is difficult to fully densify these powders (especially the irregular shaped morphology) below this temperature [9, 17].

As high temperature sintering could result in high operating cost of SPS processing of these powders, it was decided in this study to investigate the low temperature spark plasma sintering of larger particle sized irregular shaped Ti64 powders. A large particle sized powder of approximately 150 micron, which could pose more compressibility difficulties during sintering, was selected in this study as compared to some reported studies on the sintering of 10 – 100 micron size powders [9, 18, 19]. This study aims to validate the suitability of SPS technology as a viable and economical method that can be used for low temperature sintering of large particle sized Ti64 powders with irregular and angular morphology to full densification with enhanced hardness and fracture characteristics.

2 Experimental Procedure

The raw material used in this experiment was irregularly shaped Ti64 powders having a particle size of 100 mesh (approximately 150 µm), received in pre-alloyed condition from Flowmaster™. A predetermined amount of alloy powders were poured into a graphite die with a diameter of 30 mm. To prevent welding and achieve uniform current flow in the powder, thin graphite foils were placed in between powders and the graphite die. Sintering experiments followed in consecutive runs using the SPS system, model HHPD – 25 FCT Germany at a constant heating rate, uniaxially applied compaction pressure and sintering temperature of 100°C/min, 50 MPa and 850 °C respectively in a vacuum atmosphere. As the sintering experiment progressed, an optical pyrometer embedded within the upper punch and 5 mm from the sample surface was used to record the temperature within the core of the sample. Linear shrinkages of powder compacts were also monitored as a function of the relative

Journal of Engineering Technology (ISSN: 0747-9964)
Volume 6. Issue 1. Jan. 2017. PP.35-48

displacement of the graphite punch. A pre-compaction force of 10 kN was applied to create contact with the powder. The holding time during sintering was varied between 2 – 10 min. Discs of sintered samples (Ø 30 mm x 5 mm thick) were retrieved from the graphite die after each sintering run. The densities of sintered samples were measured following Archimedes' principle at a room temperature of 23°C where water density was 0.997538 g/mL. The recorded density was an arithmetic mean of five different measurements taken from each sample. The relative density of samples was calculated as a function of both the theoretical and measured densities of the sintered Ti64 alloy discs.

Micro-hardness tests were performed at room temperature on sectioned as-polished surfaces at a load of 100 gf (1.0 N) and dwell time of 15 s according to the Vickers indentation method using FUTURE – TECH FM 800 micro-hardness tester equipped with an optical microscope. The hardness result for each sample was the arithmetic mean of ten successive indentations with standard deviations. The morphology of as-received pre-alloyed Ti64 powder and microstructural characterization of as-polished sintered samples were achieved using High-Resolution Field Emission Scanning Electron Microscope (JSM-7600F, Jeol, Japan) equipped with an EDX detector (Oxford X-Max) with INCA X-stream2 pulse analyzer software and Back Scattered Electron (BSE) detectors. Imaging was performed with an electron beam accelerating voltage of 15 kV, a probe current of 0.5×10^{-9} A, a working distance of 8 mm between the sample surface and the electron beam pupil as well as a high chamber vacuum gauge of 8.7×10^{-4} Pa. The INCA analyzer software was set to 70 s acquisition time and a process time of 2 s. Phase identification and characterization studies were carried out using the X-ray diffraction analytical technique on machine model PANalytical EMPERIA with Cu Kα radiation and the results were analyzed with the High-score plus software. The polished samples were etched with Kroll's reagent (6 ml HF, 12 ml HNO_3 in 150 ml H_2O) before SEM analyses were carried out on them.

3 Results and Discussion

3.1 As-received powder characterization

The prealloyed Ti64 powder as characterized by SEM and EDS spot analysis respectively is shown in Figure 1. Figure 1 (b) shows the powder particles are irregular and angularly shaped with features of powder agglomeration, which are typical of powders produced by HDH processes. The EDS analysis (Figure 1 (c)) of the area within the white box (Figure 1 (a)) showed the prealloyed powder contained Ti, Al, and V with traces of C, Si and Cu.

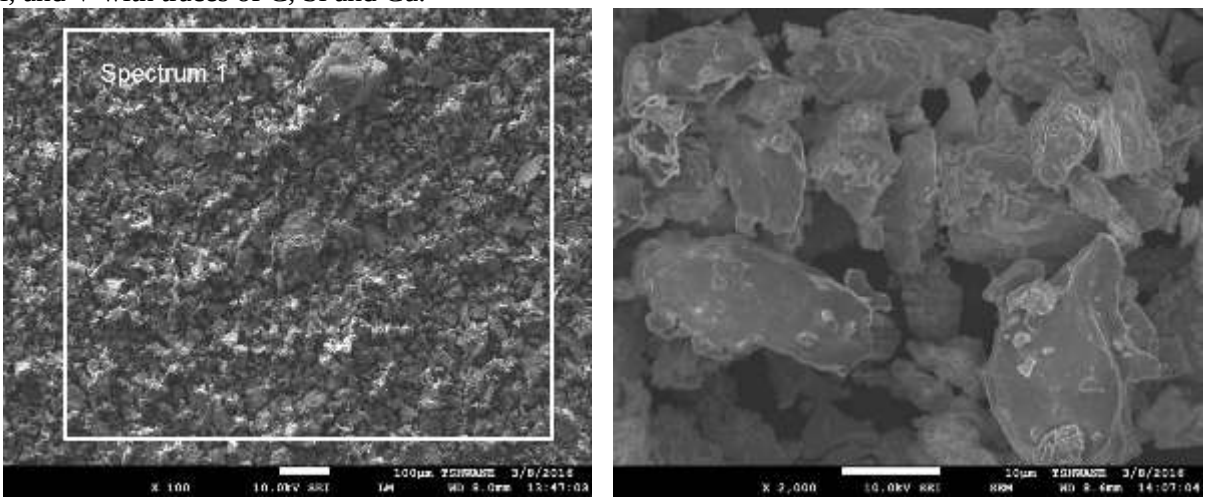

Journal of Engineering Technology (ISSN: 0747-9964)
Volume 6. Issue 1. Jan. 2017. PP.35-48

(a) (b)

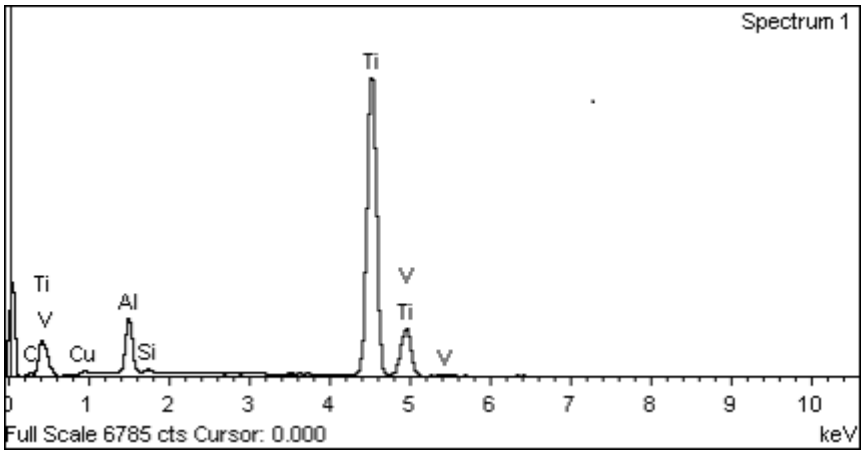

(c)

Figure. 1. SEM micrographs of as-received Ti64 powders at (a) low and (b) high magnifications, with corresponding (c) EDS spot analysis.

3.2 Densification mechanism and microstructural evolution

The sintering profile as retrieved from the SPS system is represented in Figure 2. The plot of the shrinkage against time showed four different sections which have been identified by Zhaohui *et al*. [20] and Diouf *et al*. [15] as regions of i) activation and refining of powder, ii) formation of sintering neck, iii) growth of sintering neck and iv) plastic deformation densification respectively. These identified regions (labeled a, b, c and d, separated with dotted lines on the 10 min curve (Figure 2) depict the activities occurring during a sintering process leading to the densification of the bulk material. Extensive sintering took place in the third region "c" while region "d" represents plastic deformation densification, occurring due to the application of pressure at high temperature after a substantial growth of sintering neck. All these regions are present at all the holding time levels investigated in this study, although a region may be short (or extended), early (or delayed) depending on the activities occurring during sintering at that level.

Journal of Engineering Technology (ISSN: 0747-9964)
Volume 6. Issue 1. Jan. 2017. PP.35-48

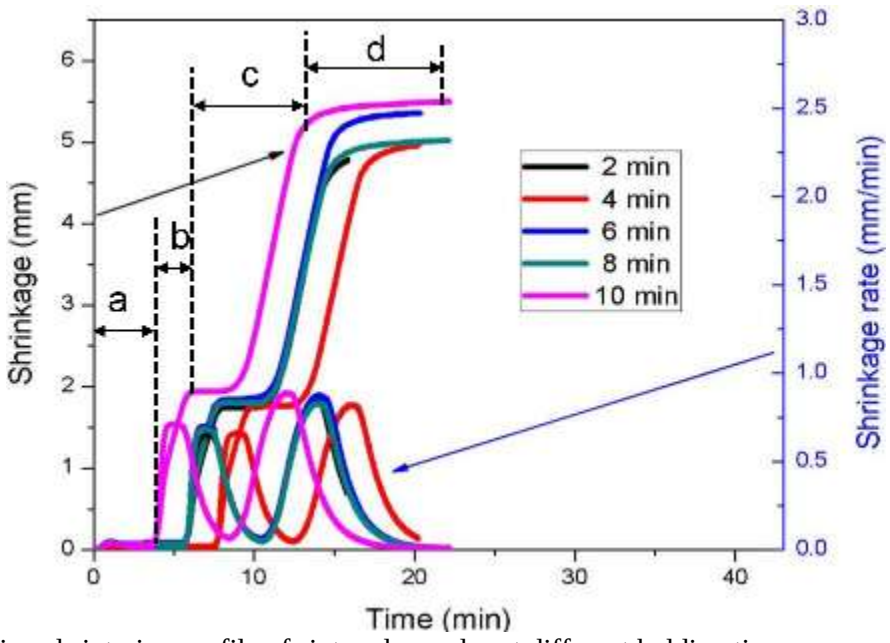

Figure. 2. Retrieved sintering profile of sintered samples at different holding times.

The highest shrinkage and shrinkage rate was observed in the sample held at sintering temperature for 10 min. This sample also showed early onset of sintering at around 4 min and had the longest plastic deformation densification region, which is why it had the highest relative density (99.9 %) as seen in Figure 3. Samples held at sintering temperature for 2, 6 and 8 min had overlapping "a", "b" and "c" regions (Figure 2) suggesting they had similar sintering mechanisms occurring in them as sintering progressed within these regions. However, they have separated plastic deformation densification regions with the shortest observed in the sample held for 2 min at sintering temperature which is partly responsible for its lowest relative density of 93.7 % (Figure 3), aside from being the sample with the lowest observed shrinkage. Experimental results showed densification improved progressively from 93.7 % to 99.9 % as holding time increased from 2 – 10 min with 6 % enhancement in densification at 10 min holding time. Beyond 6 min holding time, the associated relative densities were almost constant with minimal but non-significant changes. The sample sintered at 4 min holding time had the most delayed onset of sintering observed after 8 min into the sintering process (Figure 2).

The microstructural evolution that occurred in the sintered samples due to varied holding times is shown in Figure 4. At 2 min holding time (Figure 4 (a)), a fairly porous microstructure is seen with open pores (dark spots indicated by arrow) distributed around the microstructure with particulate features still evident therein which suggested the sample was still largely in the process of densification. This corroborates the earlier observations from the sintering profile that this sample had the lowest observed relative density. Solid phases were just beginning to form at this stage. As the holding time increased, however, the open pores began to close up and coalesce leading to the observed reduction in pore density (number of pores) and sizes (Figures 4 (b) and (c)). Here, the different phases formed are more pronounced with α – lath (lamellar) structure in colonies as shown in the closed curves. The pores had totally disappeared at 10 min holding time (Figure 4 (e)) which again supported why this sample exhibited the best densification.

Journal of Engineering Technology (ISSN: 0747-9964)
Volume 6. Issue 1. Jan. 2017. PP.35-48

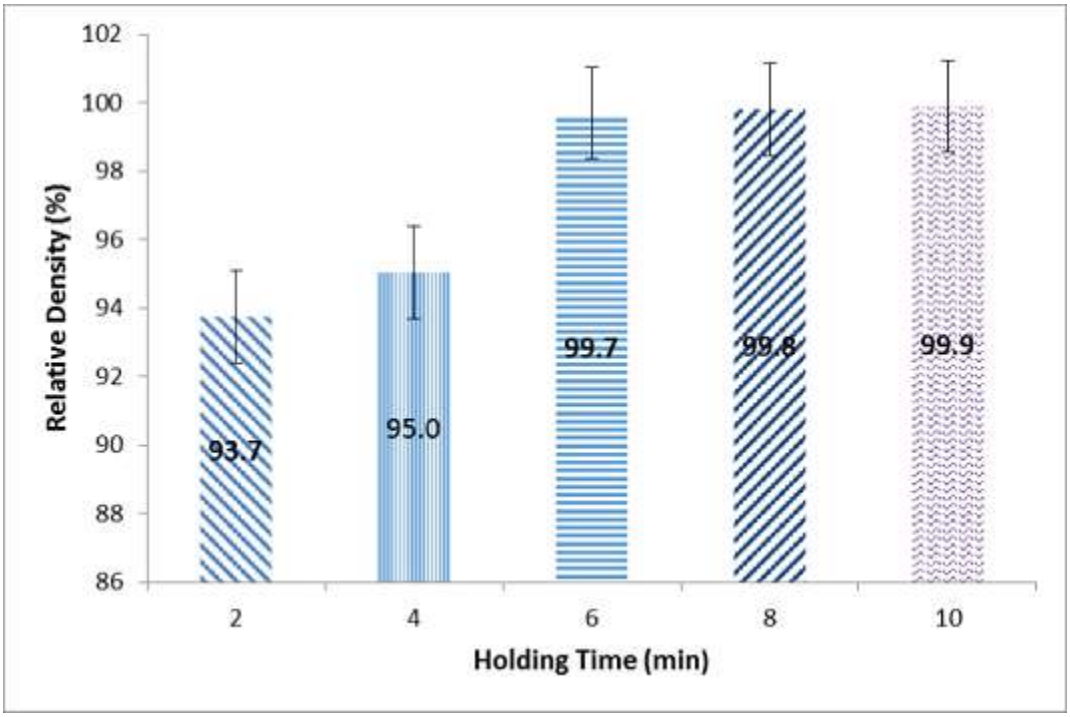

Figure. 3. Relative densities of sintered samples at different holding times.

As previously reported by Teber *et al*. [21] and Ergül *et al*. [22], pores tend to close up at high temperature due to diffusion at particle boundaries leading to grain boundary sliding and grain rotation thereby resulting in densification enhancement. Figure 4 (e) shows fully formed α (dark gray phase) and β (white phase, indicated with black arrows and mostly on α grain boundaries) in addition to the combined characteristic Ti64 bimodal (α+β) phase (also indicated with an arrow in Figure 4 (d)). These phases were fully formed at 8 and 10 min holding time respectively. Grain coarsening was also evident in these samples due to prolonged holding time at the sintering temperature. The gray areas are rich in aluminum while the white phases were stabilized by vanadium. EDS spot analysis of the different phases taken from selected sintered samples revealed the α-phase had about 6.67 wt % Al and 3.79 wt % V while the β-phase had 8.12 wt % V and 4.55 wt % respectively. These identified phases were also confirmed by the XRD patterns of the sintered alloy samples as presented in Figure 5. Peak intensities of the identified phases increased with increasing holding time and the highest intensities recorded at 10 min. There was no peak broadening noticed for all the samples.

3.3 Effects of holding time on Vickers micro-indentation hardness

Figure 6 summarizes the Vickers micro-hardness behavior of Ti64 powders sintered at varied holding times from 2 – 10 min with sintering temperature kept constant at 850 °C. It was observed that hardness increased initially as holding time increased from 2 – 6 min. However, the measured hardness values began to decrease beyond 6 min holding time and this continued until 10 min suggesting a peak in hardness was reached at 6 min. The measured average diagonal lengths of indentation "d" followed a similar pattern but in a mirror inversion image relationship trend with the microindentation hardness.

Journal of Engineering Technology (ISSN: 0747-9964)
Volume 6. Issue 1. Jan. 2017. PP.35-48

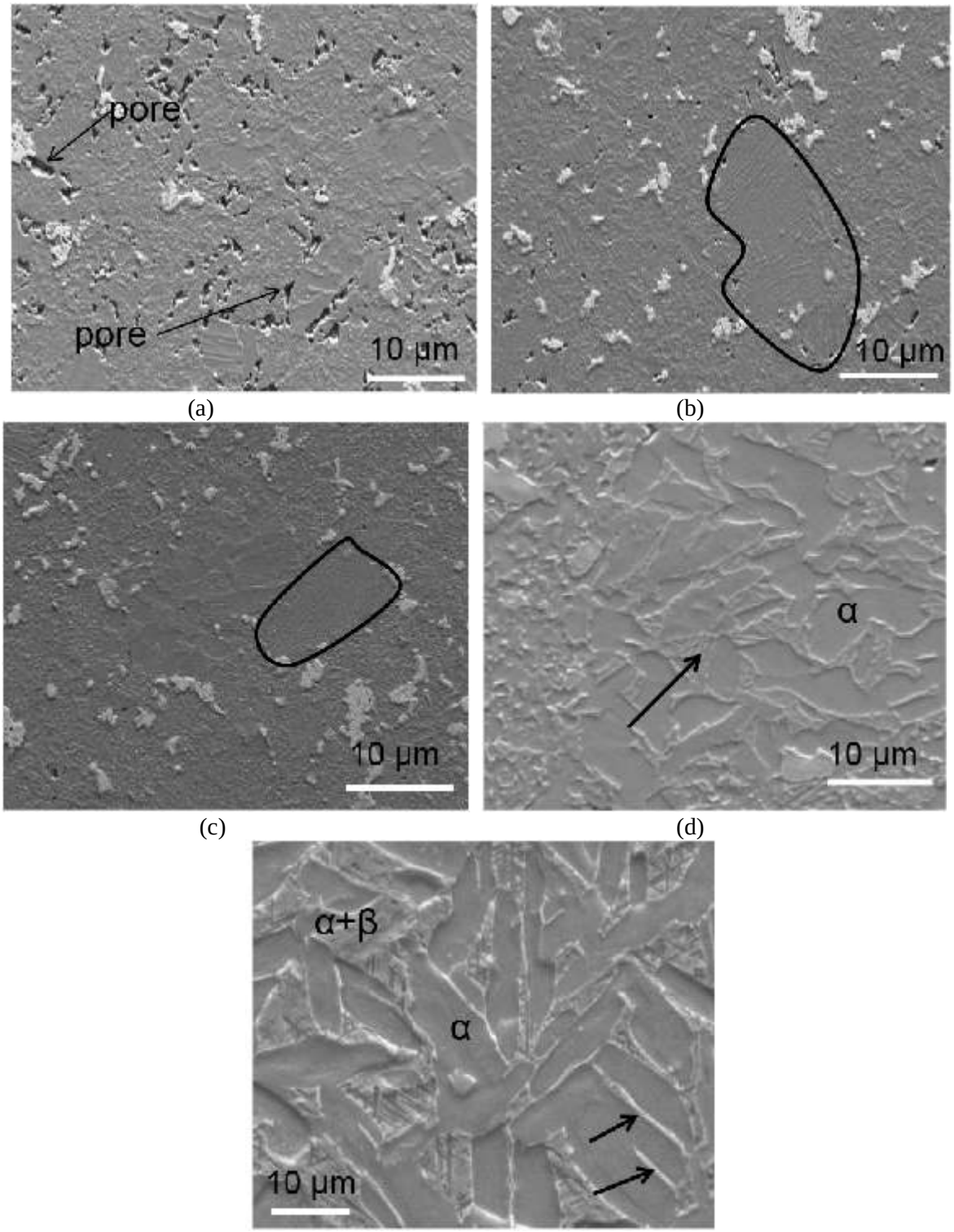

Figure. 4. SEM micrographs of Ti64 powders sinntered at varied holding times (a) 2 min (b) 4 min (c) 6 min (d) 8 min (e) 10 min.

Journal of Engineering Technology (ISSN: 0747-9964)
Volume 6. Issue 1. Jan. 2017. PP.35-48

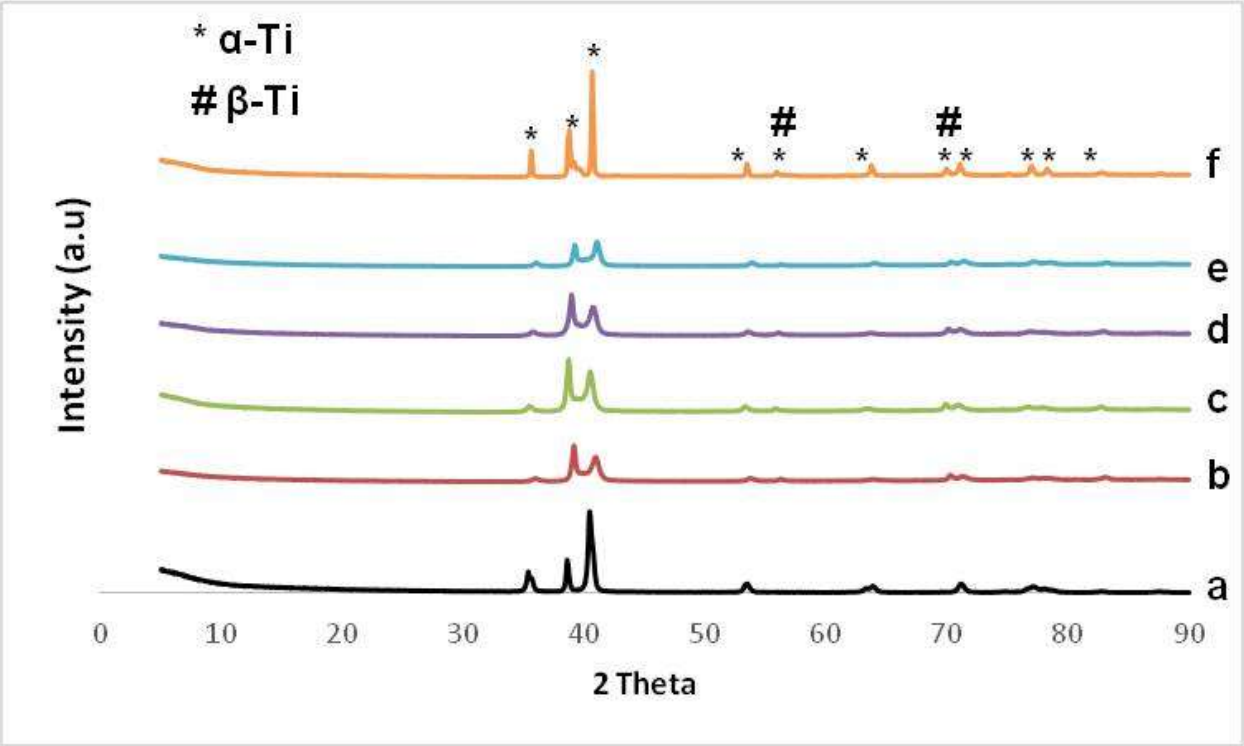

Figure. 5. XRD pattern of (a) as-received Ti64 powder and Ti64 alloys sintered at 850 °C and different holding times (b) 2 min, (c) 4 min, (d) 6 min, (e) 8 min and (f) 10 min.

This observation can be explained by the microstructural evolution of sintered samples presented in Figure 4. The initial increase in hardness up to 6 min holding time was due to the closure of open pores and the associated reduction in the pore sizes and pore density (Figures 4 (a) – (c)), as well as densification enhancement at these holding time levels (Figure 3). The drastic drop in hardness despite the absence of porosity and increasing densification with prolonged holding time at sintering temperature was assumed to be as a result of grain growth and coarsening (Figures 4 (d) – (e)). Teber et al. [21] posited in support of this position that the observed initial increase in micro-hardness was due to the homogenization of microstructure, while the decrease in the micro-hardness, on the other hand, was as a result of a sudden increase in grain size. These had a negative effect on the measured hardness values leading to 5 % deterioration in micro-hardness from 366 – 347 $HV_{0.1}$ between 6 – 10 min respectively.

The micro-hardness indentation micrographs as captured from the optical microscope attached with the micro-hardness tester is presented in Figure 7. The indentations were made on as-polished surfaces of the sintered samples before etching. A comparative study of the micrographs showed a progressive reduction in porosity with increased holding time. This also showed a positive correlation with the densification pattern in the sintered samples. A further examination was done on the micro-indentation patterns to ascertain the presence of cracks, slip modes, barreling or pincushioning, as the case may be. These have been identified as useful indicators to investigating mechanical properties and degree of densification in sintered samples [23, 24].

Journal of Engineering Technology (ISSN: 0747-9964)
Volume 6. Issue 1. Jan. 2017. PP.35-48

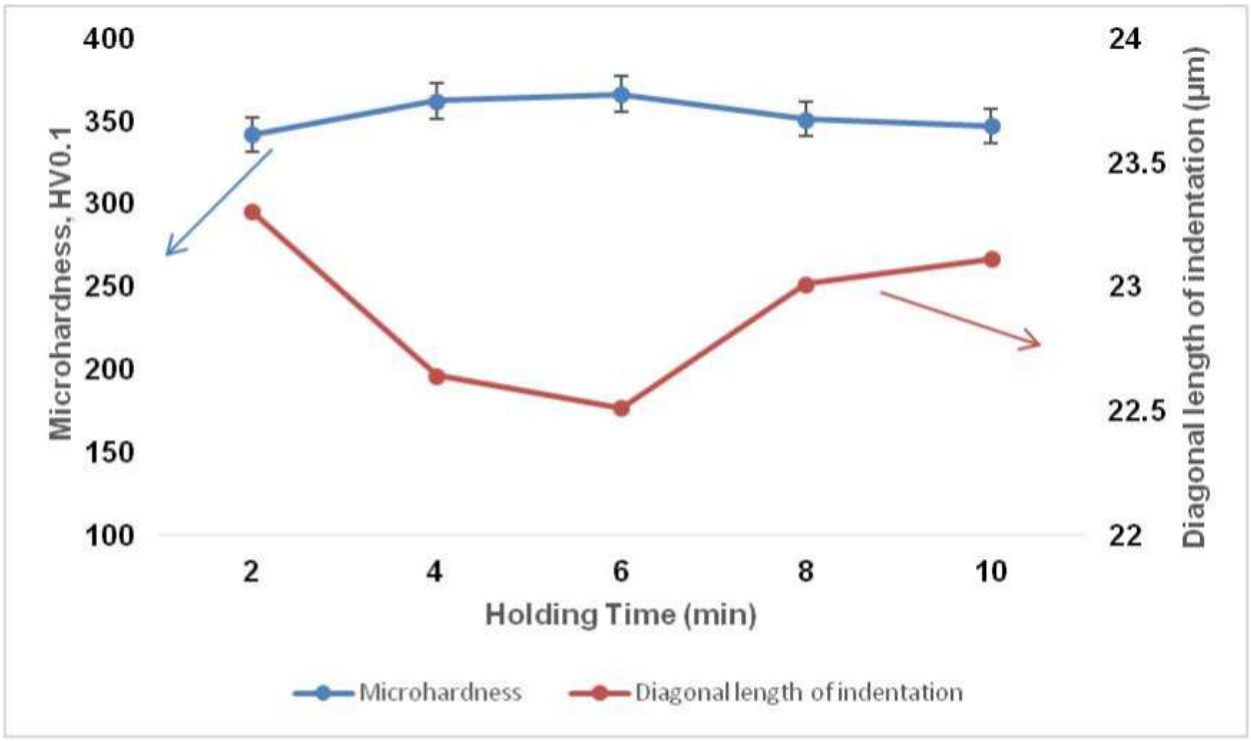

Figure. 6. Microhardness behavior of sintered samples at varied holding times

No cracks were seen in the sintered alloy samples at all the holding times investigated in this work suggesting that the samples were not brittle. The wavy slip was observed in the sample sintered at 8 min holding time which is indicative of its relative toughness and resistance to crack propagation, while the samples held for 2 and 4 min respectively at sintering temperature showed minimal barreling (bulging out of indentations) features suggesting they had poor densification around the micro-indentations. However, the samples held for 6 and 10 min at sintering temperature had no evidence of slip mode but slight pincushioning (sinking in) effects were observed indicating they possessed better densification around the micro-indentations. All these inferences made from micro-hardness indentation micrographs confirmed the earlier positions made from SEM micrographs and density measurements for all the sintered alloy samples.

3.4 Fracture surface analysis

Figure 8 shows the SEM micrographs of the fractured surfaces of samples sintered at 850 °C but at different isothermal holding times ranging from 2 – 10 min. All the fractographs had dimples on their surfaces which are typical of a ductile morphology and the occurrence of necking. However, Figures 8 (a) and (b) had some pores within the grains and there are also slightly deformed or undeformed particles which portend that the deformation in these samples is largely localized. The observed fracture mode was predominantly intergranular suggesting these samples were not well consolidated.

Journal of Engineering Technology (ISSN: 0747-9964)
Volume 6. Issue 1. Jan. 2017. PP.35-48

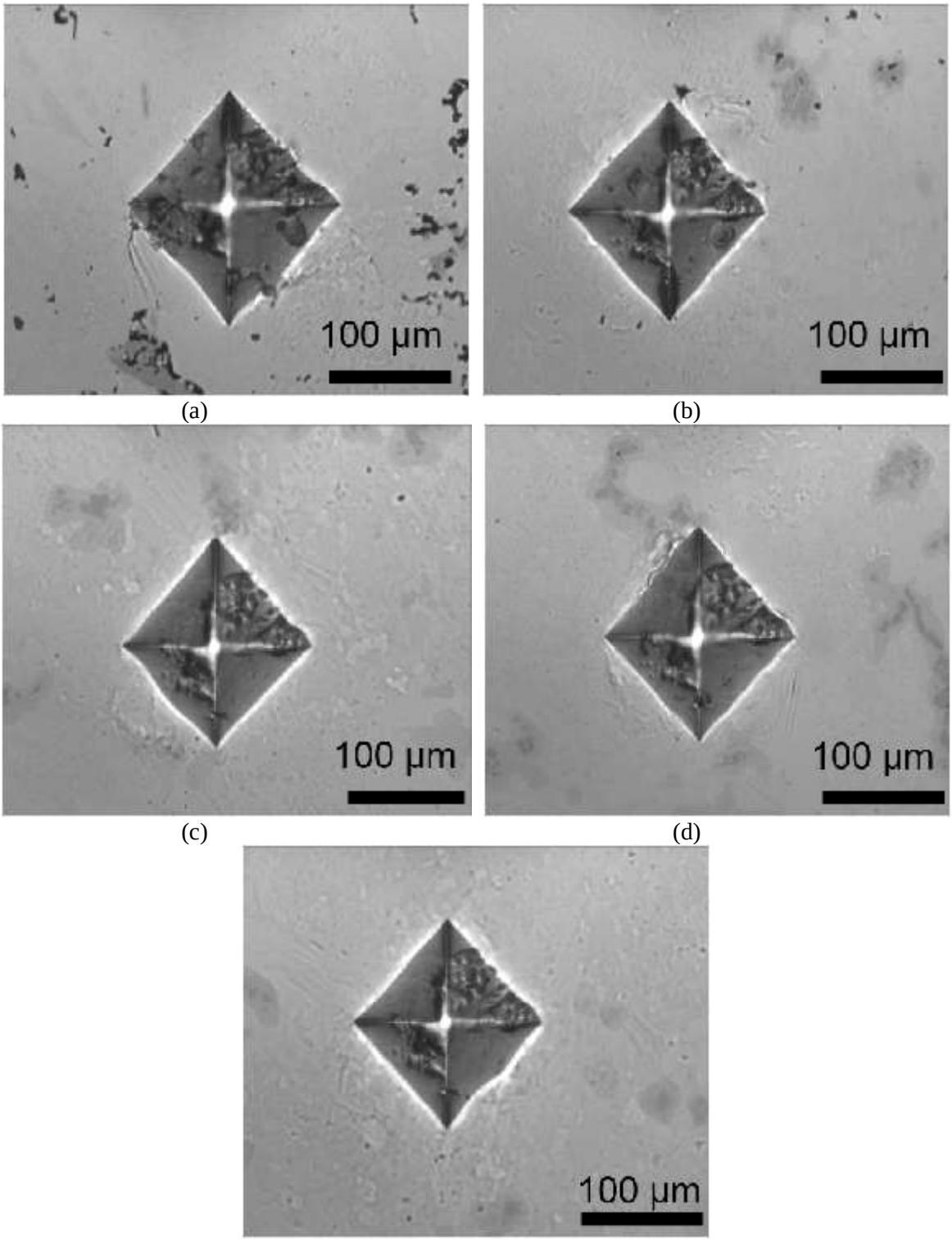

(a) (b) (c) (d) (e)

Figure. 7. Microhardness indentation micrographs for Ti64 alloys held for: (a) 2 min, (b) 4 min, (c) 6 min, (d) 8 min and (e) 10 min respectively at 850 °C sintering temperature

Journal of Engineering Technology (ISSN: 0747-9964)
Volume 6. Issue 1. Jan. 2017. PP.35-48

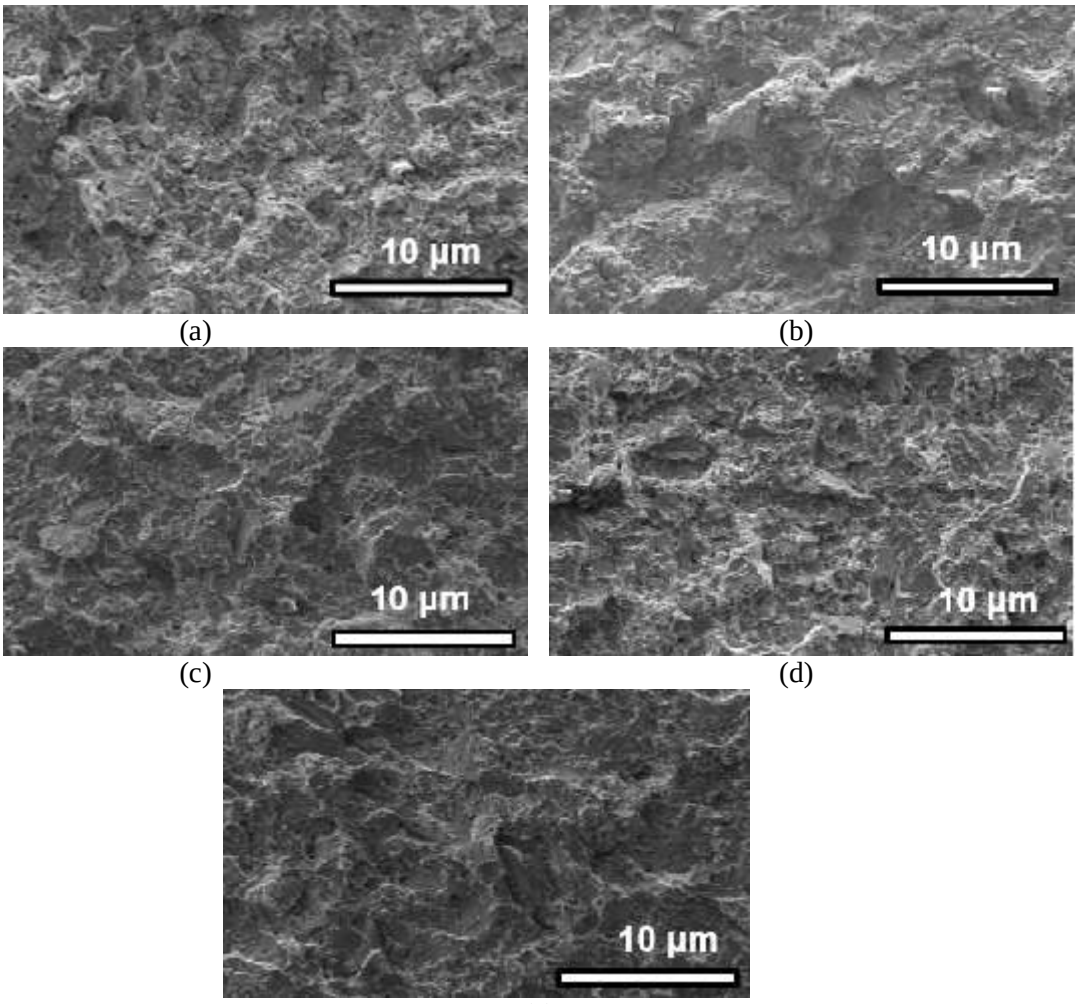

(a) (b) (c) (d) (e)

Figure. 8. SEM micrographs of fractured surfaces of Ti64 powders sintered at 850 °C and held for: (a) 2 min, (b) 4 min, (c) 6 min, (d) 8 min and (e) 10 min.

This is in agreement with the degrees of densification attained in these samples as earlier presented in Figure 3 and corroborated by the SEM micrographs of their etched, as-polished surfaces presented in Figure 4. Figures 8 (c) – (e) on the other hand showed well deformed particles and the fracture mode in these samples was purely transgranular, implying the grain boundaries had good strengths. This correlates positively with the earlier observations that these samples were well sintered and had better densification as opposed to the samples held for 2 and 4 min respectively (Figures 8 (a) and (b)) at the sintering temperature. Figures 9 (a) – (e) show the corresponding fractographs of Figure 8, presented at higher magnifications. A more critical observation on these fracture surfaces, however, revealed a decreasing amount of dimples as the holding time increased from 6 – 10 min with the least obtained in the sample held for 10 min at the sintering temperature. The implication of this is that the mechanical properties of these samples will follow a decreasing trend just as the presence of the dimples. This position also aligns with the observed decline in hardness values of the samples held for 8 and 10

Journal of Engineering Technology (ISSN: 0747-9964)
Volume 6. Issue 1. Jan. 2017. PP.35-48

min (Figure 6) respectively at sintering temperature despite their improved densifications. This was earlier attributed to the effect of abnormal grain growth as a result of prolonged holding time at the sintering temperature.

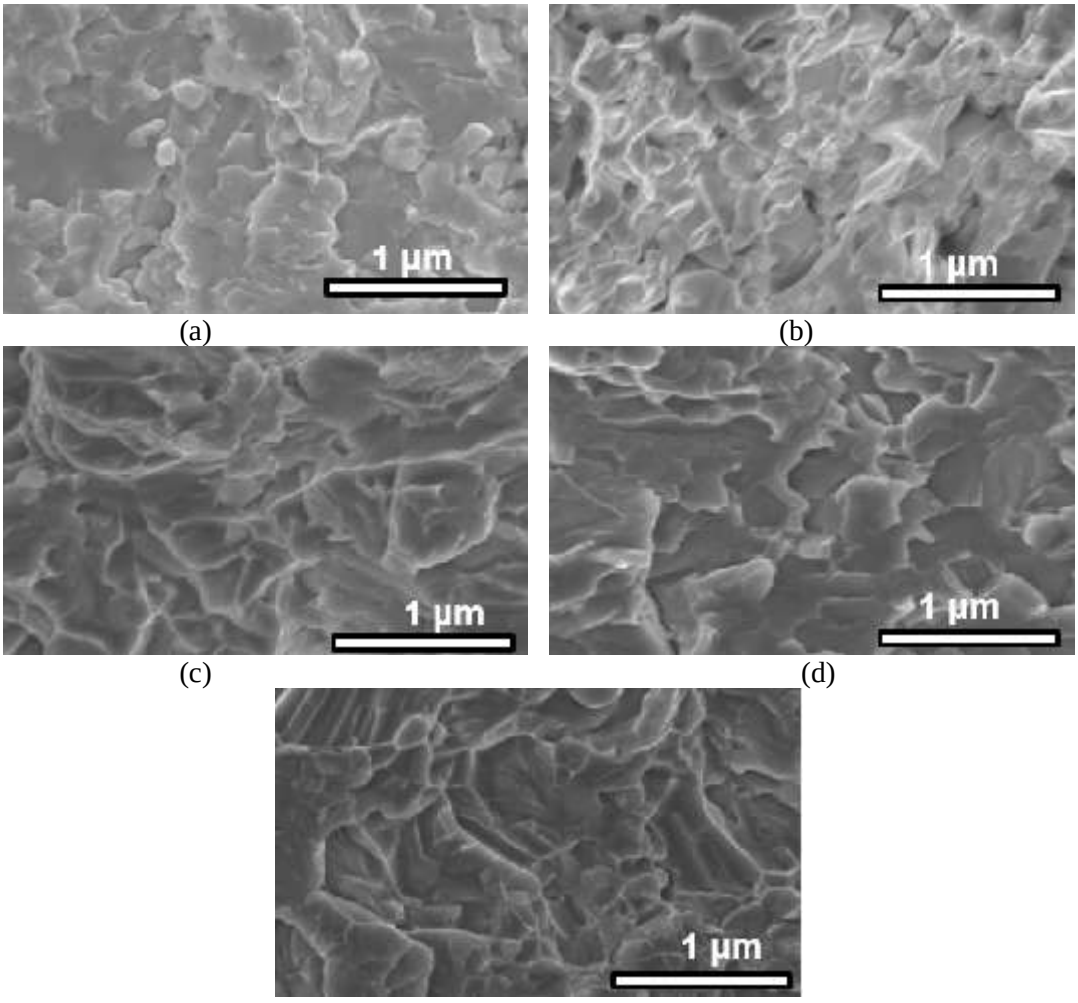

Figure. 9. Corresponding high magnification SEM micrographs for fractured surfaces of Ti64 powders sintered at 850 °C and held for: (a) 2 min, (b) 4 min, (c) 6 min, (d) 8 min and (e) 10 min respectively.

4 Conclusion

The spark plasma sintering technique and the use of a low grade feedstock powder was explored in this study, targeted at reducing the cost of producing Ti6Al4V powders into bulk materials. The results from the study showed that SPS is a viable and economical option for sintering large particle sized and irregular shaped Ti64 powders to full densification at a low temperature of 850 °C. The sintered alloy samples exhibited enhanced and impressive microstructural, hardness and fracture characteristics as obtainable from their wrought alloy counterparts produced by the conventional ingot metallurgy and other state-of-the-art technologies such as the additive manufacturing (AM) techniques. 99.7 % densification and a competitive high hardness of 366 $HV_{0.1}$ was attained at a short holding time of 6 min at sintering

Journal of Engineering Technology (ISSN: 0747-9964)
Volume 6. Issue 1. Jan. 2017. PP.35-48

temperature. Consequently, it was concluded from this study that the SPS technique is a cost-effective, time and energy saving technology for producing Ti64 bulk materials with enhanced properties.

Acknowledgments

The authors are grateful for the support of this research by Tshwane University of Technology and the Institute for NanoEngineering Research, Department of Chemical, Metallurgical and Materials Engineering, Tshwane University of Technology, South Africa.

References

[1] K. Faller, F.H. Froes, The use of titanium in family automobiles: Current trends, JOM 53(4) (2001) 27-28.
[2] N. Weston, F. Derguti, A. Tudball, M. Jackson, Spark plasma sintering of commercial and development titanium alloy powders, Journal of Materials Science 50(14) (2015) 4860-4878.
[3] F. Froes, V. Moxson, V. Duz, Titanium powder metallurgy–Automotive and more, 2004 Int Conf Powder Metallurgy & Particulate Materials, pp. 13-17.
[4] F. Froes, S. Mashl, J. Hebeisen, V. Moxson, V. Duz, The technologies of titanium powder metallurgy, JOM 56(11) (2004) 46-48.
[5] F. Froes, V. Moxson, C. Yolton, V. Duz, Titanium Powder Metallurgy in Aerospace and Automotive Components, Advances In Powder Metallurgy And Particulate Materials (9) (2003) 9-86.
[6] V.S. Moxson, O.N. Senkov, F. Froes, Production and applications of low cost titanium powder products, International Journal of Powder Metallurgy 34(5) (1998) 45-53.
[7] S. Krishnamohan, S. Ramanathan, Synthesis and Characterization of Ti6Al4V Alloy by Powder Metallurgy, International Journal of Engineering Research and Technology, ESRSA Publications, 2013.
[8] S.K. Vajpai, K. Ameyama, A novel powder metallurgy processing approach to prepare fine-grained Ti-rich TiAl-based alloys from pre-alloyed powders, Intermetallics 42 (2013) 146-155.
[9] L. Bolzoni, P. Esteban, E.M. Ruiz-Navas, E. Gordo, Influence of powder characteristics on sintering behaviour and properties of PM Ti alloys produced from prealloyed powder and master alloy, Powder Metallurgy 54(4) (2011) 543-550.
[10] H.Ö. Gülsoy, N. Gülsoy, R. Calışıcı, Particle morphology influence on mechanical and biocompatibility properties of injection molded Ti alloy powder, Bio-medical Materials and Engineering 24(5) (2014) 1861-1873.
[11] Y. Yan, G.L. Nash, P. Nash, Effect of density and pore morphology on fatigue properties of sintered Ti–6Al–4V, International Journal of Fatigue 55 (2013) 81-91.
[12] F. Lange, Sinterability of agglomerated powders, Journal of the American Ceramic Society 67(2) (1984) 83-89.
[13] C. Ouchi, H. Iizumi, S. Mitao, Effects of ultra-high purification and addition of interstitial elements on properties of pure titanium and titanium alloy, Materials Science and Engineering: A 243(1) (1998) 186-195.
[14] S. Diouf, C. Menapace, A. Molinari, Study of effect of particle size on densification of copper during spark plasma sintering, Powder Metallurgy 55(3) (2012) 228-234.
[15] S. Diouf, A. Molinari, Densification mechanisms in spark plasma sintering: Effect of particle size and pressure, Powder Technology 221 (2012) 220-227.
[16] A. Molinari, M. Zadra, Influence of the Sintering Temperature on Microstructure and Tensile Properties of Ti6Al4V Produced by Spark Plasma Sintering, EUROPM 2009 (2009) 267-272.

Journal of Engineering Technology (ISSN: 0747-9964)
Volume 6. Issue 1. Jan. 2017. PP.35-48

[17] K. Crosby, L. Shaw, C. Estournès, G. Chevallier, A.W. Fliflet, M.A. Imam, Enhancement in Ti–6Al–4V sintering via nanostructured powder and spark plasma sintering, Powder Metallurgy 57(2) (2014) 147-154.
[18] V.A.R. Henriques, P.P.d. Campos, C.A.A. Cairo, J.C. Bressiani, Production of titanium alloys for advanced aerospace systems by powder metallurgy, Materials Research 8(4) (2005) 443-446.
[19] Y. Cao, F. Zeng, J. Lu, B. Liu, Y. Liu, Y. Li, In Situ Synthesis of TiB/Ti6Al4V Composites Reinforced with Nano TiB through SPS, Materials Transactions (0) (2015).
[20] Z. Zhaohui, W. Fuchi, W. Lin, L. Shukui, S. Osamu, Sintering mechanism of large-scale ultrafine-grained copper prepared by SPS method, Materials Letters 62(24) (2008) 3987-3990.
[21] A. Teber, F. Schoenstein, F. Têtard, M. Abdellaoui, N. Jouini, Effect of SPS process sintering on the microstructure and mechanical properties of nanocrystalline TiC for tools application, International Journal of Refractory Metals and Hard Materials 30(1) (2012) 64-70.
[22] E. Ergül, H. Özkan Gülsoy, V. Günay, Effect of sintering parameters on mechanical properties of injection moulded Ti–6Al–4V alloys, Powder Metallurgy 52(1) (2009) 65-71.
[23] M.B. Shongwe, S. Diouf, M.O. Durowoju, P.A. Olubambi, Effect of sintering temperature on the microstructure and mechanical properties of Fe–30%Ni alloys produced by spark plasma sintering, Journal of Alloys and Compounds 649 (2015) 824-832.
[24] M. Chaudhri, M. Winter, The load-bearing area of a hardness indentation, Journal of Physics D: Applied Physics 21(2) (1988) 370.